ACS OMEGA

http://pubs.acs.org/journal/acsodf

Article

Kinetics and Mechanism Studies of Oxidation of Dibromothymolsulfonphthalein Toxic Dye by Potassium Permanganate in Neutral Media with the Synthesis of 2-Bromo-6-isopropyl-3-methyl-cyclohexa-2,5-dienone

Hazim M. Ali, Mohamed Abd El-Aal, Ahmed F. Al-Hossainy, and Samia M. Ibrahim*

Cite This: *ACS Omega* 2022, 7, 16109−16115

Read Online

ACCESS | Metrics & More | Article Recommendations

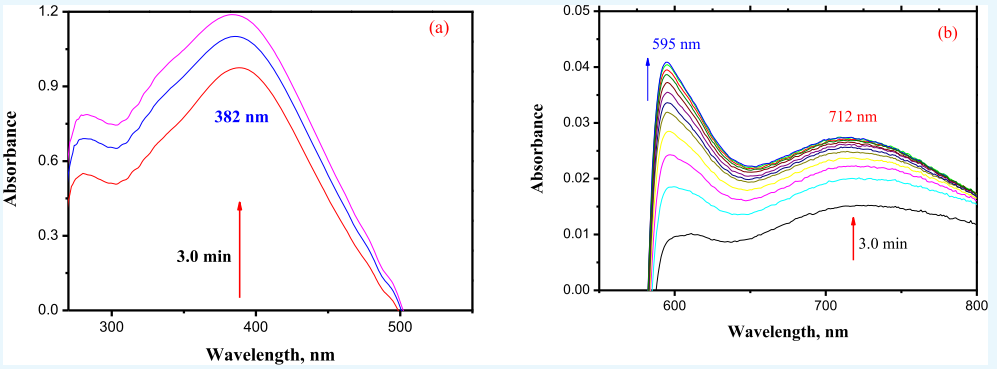

ABSTRACT: The oxidation of 3′,3″-dibromothymolsulfonphthalein (DBTS) in neutral medium by potassium permanganate multi-equivalent oxidant has been studied spectrophotometrically. Pseudo-first-order plots showed inverted S-shape throughout the entire course of the reaction. The initial rates were found to be relatively fast in the early stages, followed by a decrease in the oxidation rates over longer time periods in the slow stage. Under pseudo-first-order conditions where [DBTS] ≫ 10 [MnO_4^-], the experimental results showed a first-order dependence in [MnO_4^-] and fractional-first-order kinetics in the [DBTS] concentration. The formation of 1:1 coordination intermediate complex prior to the rate-determining step was revealed kinetically. In addition, the intermediate species involving complexes of Mn(V) coordination has been detected. The oxidation product of DBTS was identified by Fourier transform infrared spectroscopy, ultraviolet−visible spectrophotometry, and gas chromatography−mass analysis. The obtained results indicated the formation of 2-bromo-6-isopropyl-3-methyl-cyclohexa-2,5-dienone as a derivative oxidation of DBTS.

1. INTRODUCTION

Bromothymol blue (BTB) is a chemical indicator for weak acids and bases with a molecular weight of 625 g/mol and a chemical formula of $C_{27}H_{28}Br_2O_5S$. The other name of this dye is dibromothymolsulfonephthalein (DBTS). DBTS has yellowish color in acidic medium, whereas the color gradually changes from green to blue when the pH increases. The main uses of DBTS are for testing pH, as a dye for painting plant tissue, in fish breathing tanks to determine the amount of carbonic acid, in biomedical applications,[1] and in the detection of lipids and phospholipids in thin-layer chromatography. In spite of the advantages of this dye, it can cause serious problems to human being such as the stimulation of the respiratory, digestive, skin, and eye diseases.[2] The removal of this dye from wastewater has been accomplished using a variety of techniques, including adsorption, sedimentation, chemical analysis, biological method coagulation, advanced oxidation, photodegradation, and membrane separation.[3−5] However, the techniques discussed above have several drawbacks. Biological approaches, for example, take a long time to decompose complex dyes, some commercial dyes are hazardous to specific microorganisms, and the process is not reusable.[6] The creation of colloids in wastewater during the coagulation process pollutes the environment.[7] Chlorine oxidation is a slow process that necessitates the use of reactive materials that are hazardous to carry and store.[8] As a result, there is a demand for more efficient and cost-effective methods

Received: March 10, 2022
Accepted: April 19, 2022
Published: April 28, 2022

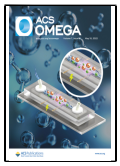

of treating textile effluents that use the least amount of chemicals and energy.

The use of various oxidants such as potassium permanganate and hydrogen peroxide for the oxidation of toxic compounds is widespread. Organic compounds with carbon−carbon double bonds, aldehyde groups, or hydroxyl groups can be oxidized by potassium permanganate. A permanganate ion, being an electrophile, is strongly attracted to the electrons in carbon−carbon double bonds found in chlorinated alkenes, borrowing electron density from these bonds to generate hypomanganate diester, a bridging, unstable oxygen compound.[9] This intermediate product undergoes additional reactions such as hydroxylation, hydrolysis, and cleavage. Potassium permanganate has various advantages, including ease of handling and the fact that it is a readily soluble solid that is particularly successful in the treatment of water and wastewater.[10] Moreover, the oxidation by permanganate ions has several different pathways and is known as a multi-equivalent oxidant.[11,12] Once again, permanganate ions were also used as an oxidizing agent to purify water from toxic organic molecules[13,14] and to test the pharmaceutical formulations' material. The kinetics of reducing permanganate ions by alcoholic polysaccharides in acidic[15,16] and alkaline solutions[17,18] have received much attention though.

The kinetics and oxidation processes of pectates,[18] methyl cellulose,[19] alginates,[20] carboxymethyl cellulose,[21] chondroitin-4-sulfate[22] carbohydrates, and BTB[23] by potassium permanganate have been studied in basic solutions. However, the oxidation of methyl cellulose,[15] pectates,[24] carboxymethyl cellulose,[25] BTB,[26] *N*-(2-acetamido)imino diacetic acid,[27] poly(ethylene glycol),[28] 2-butanol,[29,30] and mannitol[31] were investigated in acidic solutions. In these reactions, the pseudo-first-order plots were discovered to be reverse S-shape, and the reactions were found to proceed through free-radical intervention. However, to the best of our knowledge, the oxidation of DBTS dye using potassium permanganate in neutral medium has not been reported in the literature.

Therefore, the aim of the present work is the elimination of toxic DBTS coloring dye from wastewater by potassium permanganate in neutral medium using the kinetic method. The oxidation in neutral medium was found to proceed through two distinct stages. The first stage was relatively quick that was observed via a spectrophotometric detection of intermediate species involving complexes of Mn(V) coordination. The oxidation product of the cited redox reaction was identified by Fourier transform infrared spectroscopy (FTIR), ultraviolet−visible (UV−vis) spectra, and gas chromatography (GC)−mass and was found to be 2-bromo-6-isopropyl-3-methyl-cyclohexa-2,5-dienone (BIMCDO).

2. EXPERIMENTAL SECTION

2.1. Materials. All the chemicals that are used in this study are of analytical grade. Potassium permanganate ($KMnO_4$) was obtained from BDH, U.K., and DBTS was purchased from Aldrich Chemical Co. Ltd. The chemicals were dissolved in bi-distilled water to prepare the corresponding solutions. The other reagents were prepared and standardized in the same way as that mentioned previously in these papers.[32−35]

2.2. Kinetic Measurements. All kinetic measurements were performed under conditions of pseudo-first order where DBTS concentration exceeded oxidant concentration ([DBTS] ≫ 10 $[MnO_4^-]_0$). The measurements of the absorbance change were conducted on the PerkinElmer (Lambda 750) spectrophotometer using a cell path length of 1 cm. The estimation method is the same as previously used.[32,36] Figure 1

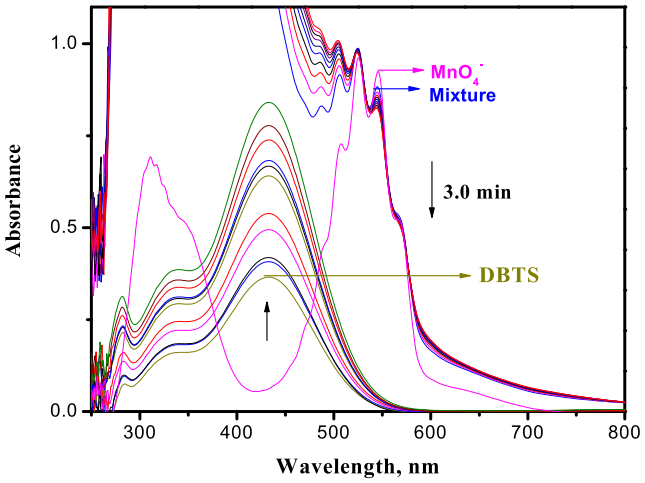

Figure 1. Spectral changes (250−800 nm) in the oxidation of DBTS by permanganate ions in neutral medium. $[MnO_4^-] = 4.0 \times 10^{-4}$ mol dm^{-3} and [DBTS] = 1.0×10^{-3} mol dm^{-3} at 25 °C.

shows the UV/vis spectrum of DBTS (1.0×10^{-3} mol dm^{-3}) oxidation by $KMnO_4$ (4.0×10^{-4} mol dm^{-3}). After the two solutions are mixed, an observed decrease in the absorption peaks of permanganate ions at 525 nm confirmed that the oxidation reaction proceeds. The decrease in the peak of permanganate ions with time is taken to monitor the progress of the oxidation reaction because it did not overlap with the other absorption peaks of other reagents in the reaction mixture. After 33 min, the MnO_4^- peak disappeared completely, which indicated the formation of some intermediates. A new peak at 382 nm, as observed in Figure 2a, revealed the formation of the intermediate complexes. With increasing the reaction time, the absorption at 595 and 710 nm increases, which indicated the formation of Mn(VI) and Mn(V) intermediate species, respectively (Figure 2b).

The absorbance−time plots revealed that the oxidation reaction was found to proceed through two separate different stages. The first stage is relatively fast, which corresponded to the development of intermediate coordination complexes [transient species of blue hypomanganate(V) and green manganate(VI)] (Figure 2b). In the second slow stage, the intermediate was slowly decomposed to produce soluble colloidal manganese(IV) and BIMCDO as an oxidation product.

2.3. Synthesis of BIMCDO. BIMCDO was synthesized by dissolving 6.24 g of the DBTS powder in 250 cm^3 of bi-distilled water. To avoid the development of aggregates, the powder was added to the solution gradually while the solution was constantly rapidly stirred. After the DBTS powder dissolved completely, the solution pH was adjusted to 7. A 250 cm^3 solution containing 1.58 g of potassium permanganate and 2 g of sodium fluoride was then added to the DBTS solution in two steps over 2 h. The reaction mixture was stirred at room temperature for 48 h, the produced MnF_4 was filtered out, and the solution was concentrated using a rotary evaporator to one-fifth of its original volume. After drying under vacuum, the obtained powder was subjected to FTIR, UV−vis spectrophotometry, and GC−mass analysis.[37−41]

https://doi.org/10.1021/acsomega.2c01462
ACS Omega 2022, 7, 16109−16115

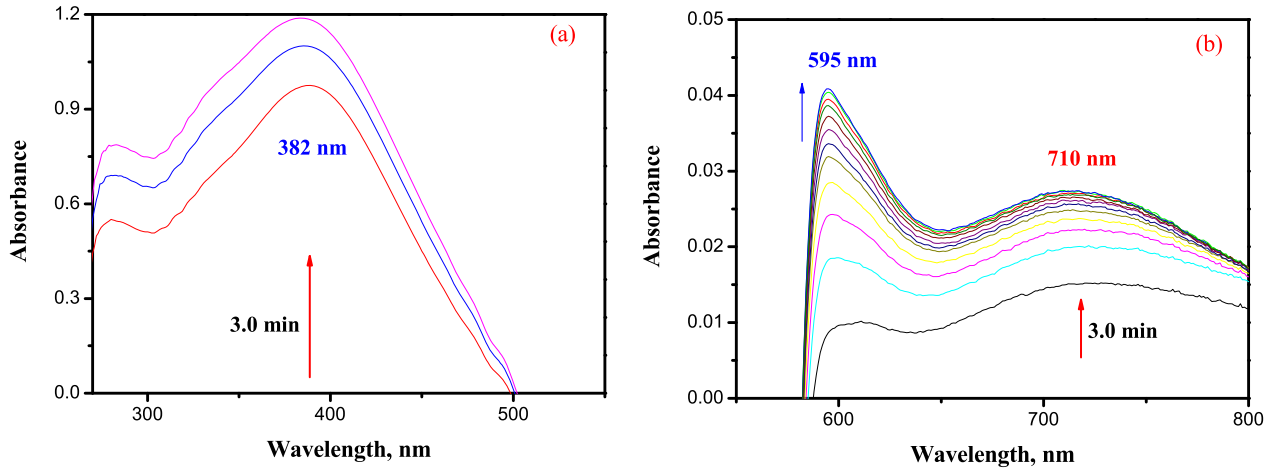

Figure 2. Spectral variations in the oxidation of DBTS by permanganate ions in neutral media. (a,b) $[MnO_4^-] = 4.0 \times 10^{-4}$ mol dm^{-3} and [DBTS] = 1.0×10^{-3} mol dm^{-3} at 25 °C (reference cell: $[MnO_4^-] = 4.0 \times 10^{-4}$ mol dm^{-3}).

3. RESULTS AND DISCUSSION

3.1. Stoichiometry. At room temperature, the oxidation reaction was proceeded with differing initial concentrations of DBTS and MnO_4^-. The unreacted permanganate ion was measured on a regular basis until a consistent value was achieved. A stoichiometric mean of 1.0 mol has been found ($[MnO_4^-]_{unreacted}/[DBTS]_0$), which agrees with the following stoichiometric equation

$$C_{27}H_{28}Br_2O_5S + HMnO_4^- = C_{10}H_{13}BrO + C_{17}H_{16}BrO_4S + MnO_2 + O_2 \quad (1)$$

where $C_{27}H_{28}Br_2O_5S$ and $C_{10}H_{13}BrO$ denote the DBTS and BIMCDO, respectively.

The FTIR spectra of DBTS and its corresponding oxidation product (BIMCDO) are shown in Figure 3 For DBTS, the main characteristic bands can be ascribed as follows: 3481 and 3443 cm^{-1} (O−H stretching vibration), 2962 and 870 cm^{-1} (C−H stretching vibrations), 1605−1556 cm^{-1} (C═C stretching modes), 1473 and 1451 cm^{-1} (C−H bending vibrations), 1404 and 1381 cm^{-1} (C−O−H bending mode), 1347, 1158, and 1040 cm^{-1} (−SO_3 group), 878 and 796 cm^{-1} (asymmetric and symmetric S−O−C stretching vibration), and 652 cm^{-1} (C−Br stretching vibrations). For BIMCDO, the characteristic bands can be assigned as follows: 3448 cm^{-1} (O−H stretching vibration), 2962 cm^{-1} (C−H stretching vibration), 1637 cm^{-1} (C═O stretching mode),[42] 1412 cm^{-1} (C−O−H bending mode), 1196 and 1021 cm^{-1} (−SO_3 group very weak band), 1140 cm^{-1} (C═O bending mode), 1089 cm^{-1} (C−O stretching mode), and 618 cm^{-1} (C−Br stretching mode). The disappearance of the band located at 3481 cm^{-1} and appearance of the band at 1637 cm^{-1} in the FTIR spectrum of BIMCDO indicated the oxidation of the secondary alcoholic hydroxyl group (−CHOH) into the keto group (C═O).

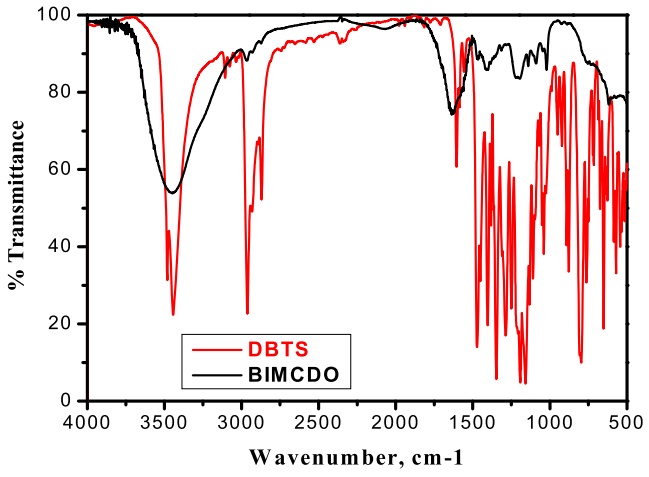

Figure 3. FTIR spectra of DBTS and its oxidation product (BIMCDO).

3.2. Curves of Dependence of Time. The relations between ln absorbance versus time is presented in Figure 4.

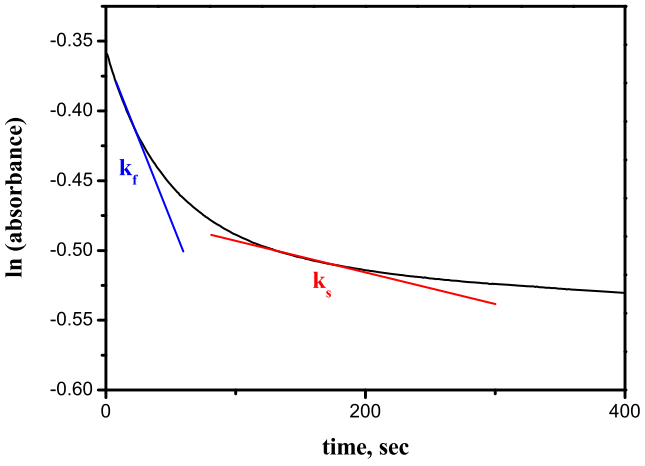

Figure 4. ln(absorbance)−time reciprocal plot in the oxidation of DBTS by permanganate ions in neutral medium. $[MnO_4^-] = 4.0 \times 10^{-4}$ mol dm^{-3} and [DBTS] = 1.0×10^{-3} mol dm^{-3} at 25 °C.

The obtained results are very unexpected, offering inverted S-shape curves showing that over the entire duration of the reaction, the oxidation kinetics are complex. The initial stage was relatively fast followed by sluggish stages with increasing the reaction time. This observation indicated that the oxidation reaction occurred over two distinct steps, involving the autoacceleration and induction processes, respectively. This

https://doi.org/10.1021/acsomega.2c01462
ACS Omega 2022, 7, 16109−16115

action may be consistent with the following term of the rate law,[25] for the species that react rapidly and slowly

$$(A_t - A_\infty) = P_0\, e^{-k_f t} + B_0\, e^{-k_s t} \quad (2)$$

where A_t is the absorbance at time t, A_∞ is the absorbance at infinity, and constants P_0 and B_0 are absorption shifts. The rate constants of the autoacceleration period can be obtained by drawing a straight line throughout the fast stage and extrapolating the line back to zero-time P_0. The k_s of the slow stage was found from plots of the relation $\ln(A_t - A_\infty)(A_\infty - A_t')$ versus time (Table 1). A typical plot is shown in Figure 4.

Table 1. Influence of Pseudo-First-Order Velocity Constants (k_{obs}) on [MnO_4^-] and [DBTS] Materials in Neutral Medium Permanganate Ion Reduction by DBTS

	$10^3 k_{obs}$, s^{-1}			$10^3 k_{obs}$, s^{-1}	
$10^4[MnO_4^-]^a$, mol dm^{-3}	k_f	k_s	$10^3[DBTS]^b$, mol dm^{-3}	k_f	k_s
2.0	1.33	0.077	1.0	1.27	0.075
4.0	1.27	0.075	2.0	1.82	0.160

[a] [DBTS] = 1×10^{-3} mol dm^{-3}. [b] [MnO_4^-] = 4×10^{-4} mol dm^{-3}. Experimental error ± 4%.

3.3. Effects of the Reaction Rate on [MnO_4^-] and [DBTS]. ln(absorbance) against time plots showed that the redox reaction in [MnO_4^-] is of first order in sequence, with good straight lines for more than two half-lives of the end of the reaction. Not only pseudo-plotting but also independent of the oxidation rates at different initial permanganate concentrations ranging from 1×10^{-4} to 5×10^{-4} mol dm^{-3} have confirmed this effect. A fractional-first-order in [DBTS] was obtained from the relationship ($\ln k_{obs} = n \ln[DBTS]$), as shown in Figure 5, where k_{obs} is pseudo-first-order rate constants for fast and slow stages (k_f and k_s), respectively. The straight lines were obtained by plots of $1/k_{obs}$ against 1/[DBTS], giving a positive intercept. The present redox system shows the creation of a 1:1 intermediate complex, as shown by Michaelis–Menten kinetics (Figure 6). The values of k_f and k_s for both fast and slow stages have been determined using the least squares method and are summarized in Table 1.

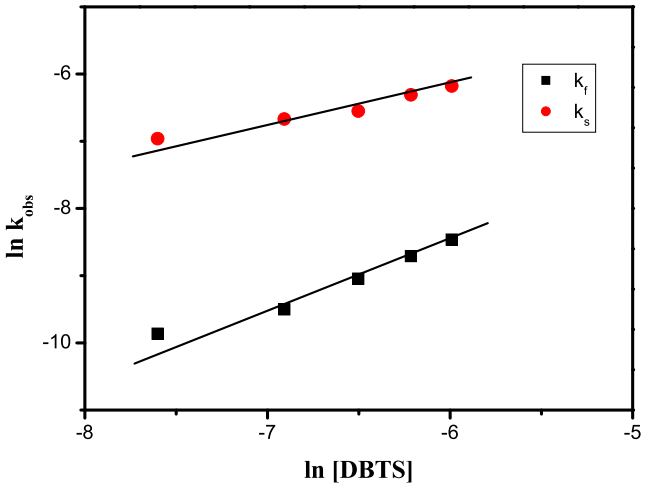

Figure 5. Plots of ln k_{obs} against ln[DBTS] in neutral medium to oxidize DBTS through potassium permanganate. [MnO_4^-] = 4.0×10^{-4} mol dm^{-3} at 25 °C.

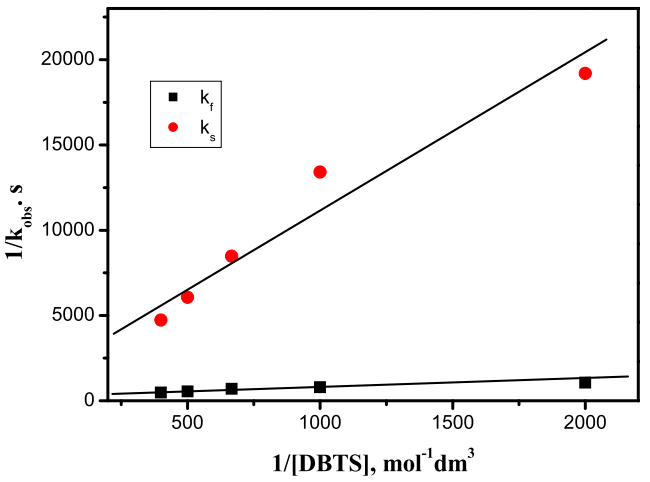

Figure 6. Plots of $1/k_{obs}$ vs 1/[DBTS] in neutral medium to oxidize DBTS through potassium permanganate. [MnO_4^-] = 4.0×10^{-4} mol dm^{-3} at 25 °C.

Although there has been a lot of research on the kinetics of permanganate ion oxidation of organic, inorganic, and alcoholic macromolecules in acidic solutions as multi-equivalent oxidants. Several problems about oxidation mechanisms in terms of electron transfer and intermediate states in rate-determining processes remain unresolved. Therefore, it is very important to know, whether the transition was carried out through a series of electron transitions (two electron transfer or more) or a sequential one-electron transfer procedure: Mn^{7+} to Mn^{6+} to Mn^{5+} in a sequence or Mn^{7+} to Mn^{5+} to Mn^{3+} in a single step. Therefore, it is important to know whether the pathways for the electron transfer process are outer-sphere or inner-sphere type.

According to the obtained kinetic results, the speculated oxidation mechanism of DBTS by permanganate ions involved attack of permanganate oxidants on the center of the substrate DBTS, giving intermediate complex (C_1). This step was followed by the formation of second intermediate complexes (C_2), which was decomposed slowly giving the final oxidation product and MnO_2, as shown in eqs 3–5.

$$DBTS + MnO_4^- \overset{K_1}{\rightleftarrows} C_1 \quad (3)$$

$$C_1 + H_2O \overset{K_2}{\rightleftarrows} C_2 \quad (4)$$

$$C_2 \overset{k}{\rightarrow} \text{product} + \text{red} \quad (5)$$

where product is the BIMCDO and red is MnO_2.

The rate constants were calculated as a function of the concentrations of substrate change using the following equation

$$\text{rate} = -\frac{d[MnO_4^-]}{dt} = \frac{kK_1K_2[DBTS]_T[MnO_4^-]}{1 + K_2[MnO_4^-]} \quad (6)$$

where $[DBTS]_T$ represents the total analytical concentration of the DBTS reducing agent. The rate-law expression is written as

https://doi.org/10.1021/acsomega.2c01462
ACS Omega 2022, 7, 16109–16115

Scheme 1. Mechanism of Oxidation of 3′,3″-Dibromothymolsulfonphthalein by Permanganate Ions in Neutral Solutions

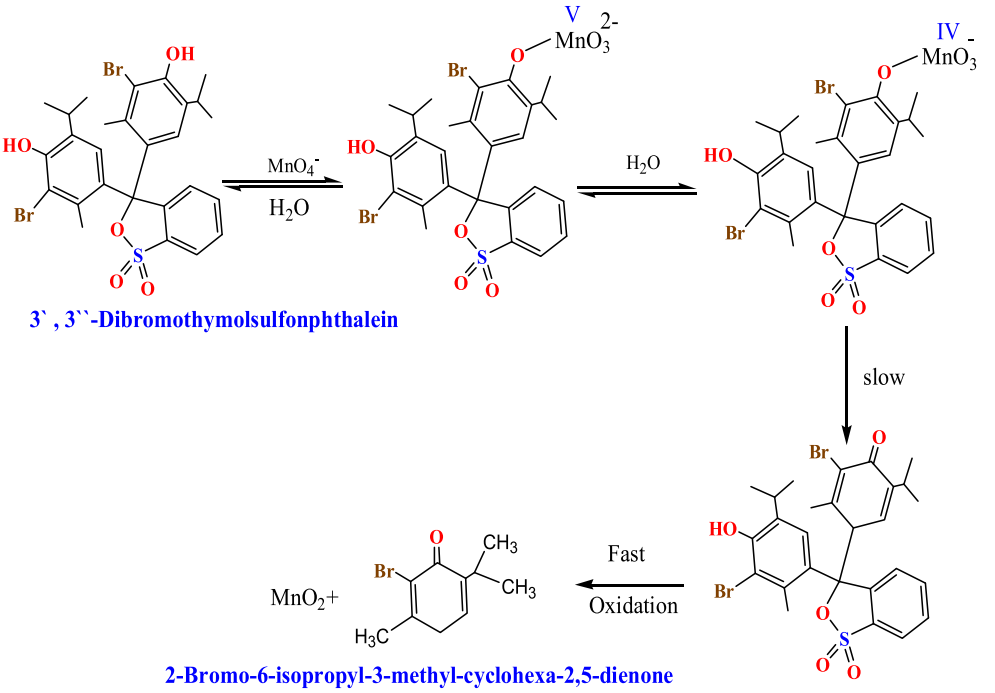

$$\text{rate} = -\frac{d[MnO_4^-]}{dt} = k_{obs}[MnO_4^-] \quad (7)$$

Comparing eqs 6 and 7 and rearrangement, the following equation was obtained

$$\frac{1}{k_{obs}} = \left(\frac{1}{kK_1K_2}\right)\frac{1}{[DBTS]} + {}^*K' \quad (8)$$

where ${}^*K' = [MnO_4^-]/kK_1[DBTS]$.

From eq 8, the plots of $(1/k_{obs})$ versus $(1/[DBTS])$ were given straight lines with positive intercepts on $(1/k_{obs})$ axes and small intercept observed in the Michaelis–Menten plot (Figure 6), and this intercept could be negligible.

The disturbance of the alteration in spectra (Figure 1) can suggest that the original quick portion of the reaction to oxidation is not the true phase of electron transfer. Therefore, the initial rapid part of oxidation may be attributed to a fast formation of an intermediate between the reactants. Moreover, several experiments have been performed to detect the hypomanganate(V) intermediate as a transient species. As seen in Figure 2b, we were able to detect intermediate Mn(V) formation, while increasing the absorption at wavelength 710 nm, which suggests the formation of intermediate Mn(V) complex. The suggested oxidation mechanism of DBTS by permanganate ions was discussed as the following: a fast attack of the permanganate oxidant on the center of the substrate, giving the intermediate complexes (C_1) $[DBTS–Mn^{V}O_4^{3-}]$ prior to the rate-determining step. Such complexation is followed by the transfer of electrons from the substrate to the oxidant in the rate-determining step to give the second intermediate complex (C_2) $[DBTS–Mn^{IV}O_4^{4-}]$ with the subtraction of H_2O through the initial fast stage of oxidation. Then, the formed Mn^{IV} reacts with the substrate to form intermediate complexes, followed by the slowly decomposed intermediate complex, giving the final oxidation product and MnO_2 (Scheme 1).

3.4. UV–Vis Spectrophotometer Characterization.

The UV–vis spectra of DBTS and BIMCDO are shown in Figure 7. The DBTS showed two peaks at λ_{max} = 276 and 430 nm, whereas the BIMCDO exhibits three absorption peaks at λ_{max} = 238, 270, and 420 nm. These results confirmed the formation of new compounds during the oxidation reaction.

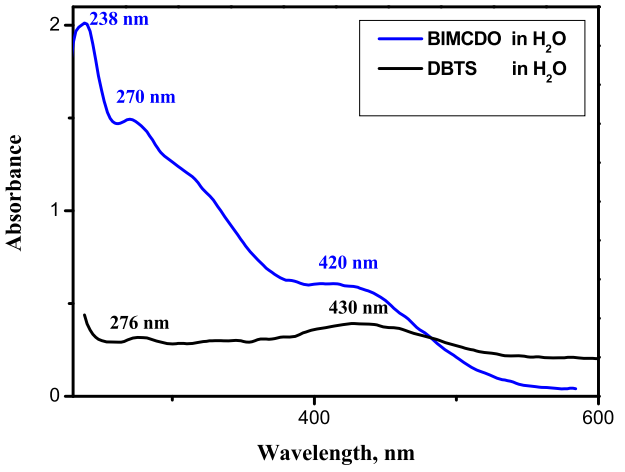

Figure 7. UV–vis spectra of DBTS and BIMCDO samples.

3.5. Mass Spectra Characterization.

GC–mass spectrum of the BIMCDO sample was recorded to confirm the oxidation product of DBTS by permanganate in neutral medium, as shown in Figure 8. The m/z = 230 suggested the formation of BIMCDO.

4. CONCLUSIONS

The oxidation of toxic 3′,3″-dibromothymolsulfonphthalein dye by MnO_4^- at pH ∼ 7 was studied using the UV–vis spectrophotometric technique. By plotting ln (absorbance) against time, the inverted S-shape curve shows that the redox

https://doi.org/10.1021/acsomega.2c01462
ACS Omega 2022, 7, 16109–16115

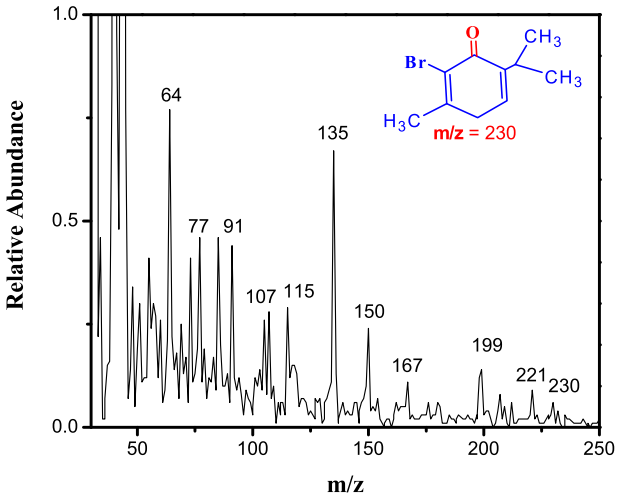

Figure 8. Mass profile of the oxidation product of DBTS (BIMCDO).

reaction occurs through two distinct stages. The first stage is relatively fast followed by decrease in the oxidation rates, called the induction period, which was shown to be linear over a longer period. Kinetic evidence for the formation of 1:1 intermediate complex has been observed. The increase in the absorption peak at λ_{max} = 710 nm is observed, suggesting the development of intermediate hypomanganate(V) as a transient compound. The oxidation product of this dye was confirmed by a variety of techniques such as such as FTIR, UV−vis, and GC−mass. Finally, the results obtained from this paper showed that it can easily remove toxic dyes form wastewater by a simple oxidation process using potassium permanganate.

AUTHOR INFORMATION

Corresponding Author

Samia M. Ibrahim − *Chemistry Department, Faculty of Science, New Valley University, El-Kharga, New Valley 72511, Egypt;* orcid.org/0000-0002-8401-2660; Email: samiamakram2001@yahoo.com, samiamakram2001@sci.nvu.edu

Authors

Hazim M. Ali − *Department of Chemistry, College of Science, Jouf University, Sakaka 72388 Aljouf, Saudi Arabia*

Mohamed Abd El-Aal − *Catalysis and Surface Chemistry Lab, Chemistry Department, Faculty of Science, Assiut University, Assiut 71516, Egypt;* orcid.org/0000-0002-8876-5977

Ahmed F. Al-Hossainy − *Chemistry Department, Faculty of Science, New Valley University, El-Kharga, New Valley 72511, Egypt*

Complete contact information is available at: https://pubs.acs.org/10.1021/acsomega.2c01462

Notes

The authors declare no competing financial interest.

ACKNOWLEDGMENTS

This work was funded by the Deanship of Scientific Research at the Jouf University under grant no. (DSR-2021-03-0349).

REFERENCES

(1) Bazbouz, M.; Tronci, G. Two-Layer Electrospun System Enabling Wound Exudate Management and Visual Infection Response. *Sensors* **2019**, *19*, 991.

(2) Bahrami, M.; Nezamzadeh-Ejhieh, A. Effect of the Supported ZnO on Clinoptilolite Nano-Particles in the Photodecolorization of Semi-Real Sample Bromothymol Blue Aqueous Solution. *Mater. Sci. Semicond. Process.* **2015**, *30*, 275−284.

(3) Lubbad, S. H.; Abu Al-Roos, B. K.; Kodeh, F. S. Adsorptive-Removal of Bromothymol Blue as Acidic-Dye Probe from Water Solution Using Latvian Sphagnum Peat Moss: Thermodynamic Assessment, Kinetic and Isotherm Modeling. *Curr. Green Chem.* **2019**, *6*, 53.

(4) Bayramoglu, M.; Kobya, M.; Can, O. T.; Sozbir, M. Operating Cost Analysis of Electrocoagulation of Textile Dye Wastewater. *Sep. Purif. Technol.* **2004**, *37*, 117−125.

(5) Can, O. T.; Kobya, M.; Demirbas, E.; Bayramoglu, M. Treatment of the Textile Wastewater by Combined Electro-coagulation. *Chemosphere* **2006**, *62*, 181−187.

(6) Pirkarami, A.; Olya, M. E. Removal of Dye from Industrial Wastewater with an Emphasis on Improving Economic Efficiency and Degradation Mechanism. *J. Saudi Chem. Soc.* **2017**, *21*, S179−S186.

(7) Ahmed Basha, C.; Bhadrinarayana, N. S.; Anantharaman, N.; Meera Sheriffa Begum, K. M. Heavy Metal Removal from Copper Smelting Effluent Using Electrochemical Cylindrical Flow Reactor. *J. Hazard. Mater.* **2008**, *152*, 71−78.

(8) Daneshvar, N.; Ashassi Sorkhabi, H.; Kasiri, M. B. Decolorization of Dye Solution Containing Acid Red 14 by Electrocoagulation with a Comparative Investigation of Different Electrode Connections. *J. Hazard. Mater.* **2004**, *112*, 55−62.

(9) Abdullah, N.; Aziz, H. A.; Yusuf, N. N. A. N.; Umar, M.; Amr, S. S. A. Potential of KMnO4 and H2O2 in Treating Semi-Aerobic Landfill Leachate. *Appl. Water Sci.* **2014**, *4*, 303−309.

(10) Xu, X.-R.; Li, H.-B.; Wang, W.-H.; Gu, J.-D. Decolorization of Dyes and Textile Wastewater by Potassium Permanganate. *Chemosphere* **2005**, *59*, 893−898.

(11) Sar, P.; Saha, B. Potential Application of Micellar Nanoreactor for Electron Transfer Reactions Mediated by a Variety of Oxidants: A Review. *Adv. Colloid Interface Sci.* **2020**, *284*, 102241.

(12) Hicks, K. W. Kinetics of the Permanganate Ion-Potassium Octacyanomolybdate(IV) Reaction. *J. Inorg. Nucl. Chem.* **1976**, *38*, 1381−1383.

(13) Liu, C. S.; Shih, K.; Wang, F. Oxidative Decomposition of Perfluorooctanesulfonate in Water by Permanganate. *Sep. Purif. Technol.* **2012**, *87*, 95−100.

(14) Guan, X.; He, D.; Ma, J.; Chen, G. Application of Permanganate in the Oxidation of Micropollutants: A Mini Review. *Front. Environ. Sci. Eng. China* **2010**, *4*, 405−413.

(15) Hassan, R.; Dahy, A. R.; Ibrahim, S.; Zaafarany, I.; Fawzy, A. Oxidation of Some Macromolecules. Kinetics and Mechanism of Oxidation of Methyl Cellulose Polysaccharide by Permanganate Ion in Acid Perchlorate Solutions. *Ind. Eng. Chem. Res.* **2012**, *51*, 5424−5432.

(16) Hassan, R. M.; Ibrahim, S. M.; Khairou, K. S. Kinetics and Mechanism of Oxidation of Pyruvate by Permanganate Ion in Aqueous Perchlorate Solution. *Transit. Met. Chem.* **2018**, *43*, 683−691.

(17) Hassan, R. M. Alginate Polyelectrolyte Ionotropic Gels. XVIII. Oxidation of Alginate Polysaccharide by Potassium Permanganate in Alkaline Solutions: Kinetics of Decomposition of Intermediate Complex. *J. Polym. Sci., Part A: Polym. Chem.* **1993**, *31*, 1147−1151.

(18) Khairou, K. S.; Hassan, R. M. Pectate Polyelectrolyte Ionotropic Gels: 1. Kinetics and Mechanisms of Formation of Manganate (VI)−Pectate Intermediate Complex during the Oxidation of Pectate Polysaccharide by Alkaline Permanganate. *Eur. Polym. J.* **2000**, *36*, 2021−2030.

(19) Shaker, A. M.; El-Khatib, R. M.; Mahran, H. S. Kinetics and Mechanism of the Decay of Methyl Cellulose-Manganate(VI) Polysaccharide Transient Species−Novel Spectrophotometric Kinetic

https://doi.org/10.1021/acsomega.2c01462
ACS Omega 2022, 7, 16109−16115

Trace of Methyl Cellulose Hypomangate(V) Gel Intermediate Polysaccharide. *J. Appl. Polym. Sci.* **2007**, *106*, 2668−2674.
(20) Hassan, R. M. Alginate Polyelectrolyte Ionotropic Gels. XIV. Kinetics and Mechanism of Formation of Intermediate Complex during the Oxidation of Alginate Polysaccharide by Alkaline Permanganate with a Spectrophotometric Evidence of Manganate-(VI) Transient Species. *J. Polym. Sci., Part A: Polym. Chem.* **1993**, *31*, 51−59.
(21) Shaker, A. M. Base-Catalyzed Oxidation of Carboxymethyl-Cellulose Polymer by Permanganate: 1. Kinetics and Mechanism of Formation of a Manganate(VI) Transient Species Complex. *J. Colloid Interface Sci.* **2001**, *233*, 197−204.
(22) Zaafarany, I. Z.; Gobouri, A.; Hassan, R. Oxidation of Some Sulfated Carbohydrates: Kinetics and Mechanism of Oxidation of Chondroitin-4-Sulfate by Alkaline Permanganate with Novel Synthesis of Coordination Biopolymer Precursor. *J. Mater. Sci. Res.* **2013**, *2*, 23−36.
(23) Al-Hossainy, A. F.; Ibrahim, S. M. Oxidation Process and Kinetics of Bromothymol Blue by Alkaline Permanganate. *Int. J. Chem. Kinet.* **2021**, *53*, 675.
(24) Abdel-Hamid, M. I.; Khairou, K. S.; Hassan, R. M. Kinetics and Mechanism of Permanganate Oxidation of Pectin Polysaccharide in Acid Perchlorate Media. *Eur. Polym. J.* **2003**, *39*, 381−387.
(25) Hassan, R. M.; Abdel-Kader, D. A.; Ahmed, S. M.; Fawzy, A.; Zaafarany, I. A.; Asghar, B. H.; Takagi, H. D. Acid-Catalyzed Oxidation of Carboxymethyl Cellulose. Kinetics and Mechanism of Permanganate Oxidation of Carboxymethyl Cellulose in Acid Perchlorate Solutions. *Catal. Commun.* **2009**, *11*, 184−190.
(26) Ibrahim, S. M.; Al-Hossainy, A. F. Kinetics and Mechanism of Oxidation of Bromothymol Blue by Permanganate Ion in Acidic Medium: Application to Textile Industrial Wastewater Treatment. *J. Mol. Liq.* **2020**, *318*, 114041.
(27) Hassan, R.; Ibrahim, S. M. Kinetics and Mechanism of Permanganate Oxidation of ADA in Aqueous Perchlorate Solutions. *Curr. Organocatal.* **2019**, *6*, 52−60.
(28) Hassan, R.; Ibrahim, S.; Sayed, S. Kinetics and Mechanistic Aspects on Electron-Transfer Process for Permanganate Oxidation of Poly(Ethylene Glycol) in Aqueous Acidic Solutions in the Presence and Absence of Ru(III) Catalyst. *Int. J. Chem. Kinet.* **2018**, *50*, 775−783.
(29) Ghosh, A.; Sengupta, K.; Saha, R.; Saha, B. Effect of CPC Micelle on N-Hetero-Aromatic Base Promoted Room Temperature Permanganate Oxidation of 2-Butanol in Aqueous Medium. *J. Mol. Liq.* **2014**, *198*, 369−380.
(30) Bhattacharyya, P.; Ghosh, A.; Saha, B. Room Temperature Micellar Catalysis on Permanganate Oxidation of Butanol to Butanal in Aqueous Medium at Atmospheric Pressure. *Tenside, Surfactants, Deterg.* **2015**, *52*, 36−40.
(31) Ghosh, A.; Datta, I.; Ghatak, S.; Mahali, K.; Bhattacharyya, S. S.; Saha, B. Picolinic Acid Promoted Permanganate Oxidation of D-Mannitol in Micellar Medium. *Tenside, Surfactants, Deterg.* **2016**, *53*, 332−346.
(32) Al-Hossainy, A. A.; Ibrahim, A.; Mogharbel, R. T.; Ibrahim, S. M. Synthesis of Novel Keto-Bromothymol Blue in Different Media Using Oxidation−Reduction Reactions: Combined Experimental and DFT-TDDFT Computational Studies. *Chem. Pap.* **2021**, *75*, 3103−3118.
(33) Almutlaq, N.; Al-Hossainy, A. F. Novel Synthesis, Structure Characterization, DFT and Investigation of the Optical Properties of Diphenylphosphine Compound/Zinc Oxide [DPPB+ZnO]C Nanocomposite Thin Film. *Compos. Interfaces* **2021**, *28*, 879−904.
(34) Ibrahim, S. M.; Bourezgui, A.; Al-Hossainy, A. F. Novel Synthesis, DFT and Investigation of the Optical and Electrical Properties of Carboxymethyl Cellulose/Thiobarbituric Acid/Copper Oxide [CMC + TBA/CuO]C Nanocomposite Film. *J. Polym. Res.* **2020**, *27*, 264.
(35) Al-Hossainy, A. F.; Abdelaal, R. M.; Sayed, W. N. E. El. Novel Synthesis, Structure Characterization, DFT and Investigation of the Optical Properties of Cyanine Dye/Zinc Oxide [4-CHMQI/ZnO]C Nanocomposite Thin Film. *J. Mol. Struct.* **2021**, *1224*, 128989.
(36) Manhas, M. S.; Mohammed, F.; khan, Z. A Kinetic Study of Oxidation of β-Cyclodextrin by Permanganate in Aqueous Media. *Colloids Surf., A* **2007**, *295*, 165−171.
(37) Al-Hossainy, A. A. Combined Experimental and TDDFT-DFT Computation, Characterization, and Optical Properties for Synthesis of Keto-Bromothymol Blue Dye Thin Film as Optoelectronic Devices. *J. Electron. Mater.* **2021**, *50*, 3800−3813.
(38) Ibrahim, S. M.; Saad, N.; Ahmed, M. M.; Abd El−Aal, M. Novel Synthesis of Antibacterial Pyrone Derivatives Using Kinetics and Mechanism of Oxidation of Azithromycin by Alkaline Permanganate. *Bioorg. Chem.* **2022**, *119*, 105553.
(39) Hassan, R. M.; Ibrahim, S. M.; Ahmed, F. Novel Synthesis of Coordination Bipolymer Precursors of Sulfated Macromolecules as Alternative Promising in Biomedicine, Pharmaceutics and Engineering Industry by Oxidation of Sustainable and Biodegradable Sulfated Iota-Carrageenan by Alkaline Permanganat. *J. Nanomed.* **2020**, *3*, 1026.
(40) Hassan, R. M.; Ibrahim, S. M. Novel Synthesis of Coordination Biopolymer Precursor from Oxidation of Methyl Cellulose by Alkaline Potassium Permanganate. *Integr.Food, Nutr.Metab.* **2019**, *6*, 1−5.
(41) Hassan, R. M.; Ibrahim, S. M.; Khairou, K. S. Novel Synthesis of Diketopectate Coordination Biopolymer Derivatives as Journal of Nutrition and Food Processing. *J.Nutr.Food Process.* **2019**, *2*, 1−5.
(42) Sar, P.; Roy, S. G.; De, P.; Ghosh, S. Synthesis of Glutamic Acid Derived Organogels and Their Applications in Dye Removal from Aqueous Medium. *Macromol. Mater. Eng.* **2020**, *305*, 1900809.

https://doi.org/10.1021/acsomega.2c01462
ACS Omega 2022, 7, 16109−16115